Robust Output Feedback Variable-Horizon MPC with Adaptive Terminal Constraints

Renato Quartullo, Gianni Bianchini, Andrea Garulli, Antonio Giannitrapani

***Abstract*— This letter presents a robust output feedback variable-horizon model predictive control scheme for systems in which the state is not directly available but is estimated from noisy measurements. The control scheme is designed to intercept a moving target with a known trajectory while ensuring constraint satisfaction, recursive feasibility and finite-time convergence in the presence of bounded process disturbances and measurement noise. A key novelty of the proposed approach is the online adaptation of the terminal set, which reduces conservatism and improves performance in terms of final distance to the target, compared to existing tube-based methods. The effectiveness of the proposed approach is demonstrated on a numerical example concerning an orbital rendezvous maneuver of a spacecraft with an uncontrolled rotating object.**

I. Introduction

Model predictive control (MPC) is widely used in constrained control problems due to its ability to optimize performance while respecting system limitations. Traditional MPC relies on solving an optimal control problem at each time step, where the cost function depends on the state and input variables over a fixed-length prediction horizon [1]. Recently, approaches that consider the horizon length as a problem variable have gained attention, as this enables greater flexibility in the optimization problem and allows tasks to be completed within prescribed deadlines. Several techniques directly minimize the horizon length, as in time-optimal MPC [2]–[6], while others, like shrinking-horizon MPC, reduce it step by step [7], [8]. An even more flexible framework is *Variable-Horizon MPC* (VH-MPC), in which the horizon length is included among the optimization variables in the cost function. Introduced in [9] for linear systems with bounded disturbances, this approach ensures recursive feasibility, finite-time convergence and robust constraint satisfaction via tube-based MPC. However, its level of conservatism depends on the choice of the terminal constraint. In this respect, an adaptive terminal constraint selection is adopted in [10], whose aim is to minimize the final distance to a reference trajectory.

The aforementioned approaches rely on state feedback, assuming full knowledge of the system state. In many practical scenarios, only partial knowledge of the state is available, possibly corrupted by noise. This introduces the necessity to incorporate state estimation to ensure feasibility and robustness against disturbances. A possible solution is to resort to output feedback tube-based MPC. In [11], [12], tube-based MPC is combined with state estimation performed via a Luenberger observer, while [13] extends this approach to handle time-varying constraints. Meanwhile, alternative estimation techniques, such as set-membership methods, have been explored to enhance robustness [14]–[16]. All these approaches focus on fixed-horizon optimal control problems. To the best of our knowledge, output feedback tube-based MPC schemes relying on variable-horizon formulations have not been explored so far.

In this letter, a robust output feedback VH-MPC scheme with adaptive terminal constraints is proposed, in which the state is estimated through a Luenberger observer from noisy measurements. The goal is to intercept a moving target with a known trajectory, in the presence of bounded process disturbance and measurement noise. The main novelty is the introduction of an adaptive mechanism for setting the terminal constraint set, following the approach in [10], to cope with the output feedback case. This solution has the twofold objective of preserving recursive feasibility and finite-time convergence while reducing as much as possible the final distance to the target, despite the lack of full state information. The proposed output feedback VH-MPC scheme is validated on a numerical example involving an orbital rendezvous maneuver of a spacecraft with an uncontrolled tumbling object.

The rest of the letter is organized as follows. The output feedback control problem is introduced in Section II. The proposed MPC scheme is presented in Section III, along with a discussion of its properties. Simulation results are reported in Section IV. Some conclusions are drawn in Section V.

The adopted notation is fairly standard. The symbols $\oplus$ and $\ominus$ represent the Minkowski sum and Pointryagin set difference, respectively. The notation $\lfloor c \rfloor$ is used to indicate the integer part of $c \in \mathbb{R}$.

II. Tube-based Output Feedback Control

Let us consider the discrete-time linear time-invariant system

$$\begin{aligned} x(k+1) &= Ax(k) + Bu(k) + w(k), \\ y(k) &= Cx(k) + n(k), \end{aligned} \tag{1}$$

where $x(k) \in \mathbb{R}^n$ is the system state at time k, $u(k) \in \mathbb{R}^m$ is the control input, $y(k) \in \mathbb{R}^p$ is the measured output, and $w(k)$ and $n(k)$ are the process disturbance and measurement noise, respectively. It is assumed that $w(k)$ and $n(k)$ are bounded, i.e. $w(k) \in \mathcal{W}$, $n(k) \in \mathcal{N}$, where $\mathcal{W}$ and $\mathcal{N}$ are bounded

Dipartimento di Ingegneria dell'Informazione e Scienze Matematiche, Università di Siena, Italy. Email: {quartullo,giannibi,garulli,giannitrapani}@diism.unisi.it.

convex sets containing the origin. The control objective is to drive the state to a small neighborhood of a known reference trajectory $r(k)$ in finite time, while optimizing a suitable performance index. Moreover, system (1) is subject to the following (possibly time-varying) state and input constraints

$$x(k) \in \mathcal{X}(k), \quad u(k) \in \mathcal{U}(k). \tag{2}$$

The sets $\mathcal{X}(k)$ and $\mathcal{U}(k)$ are assumed to be convex and to contain the origin. Moreover, the pairs (A, B) and (A, C) are stabilizable and detectable, respectively. Hereafter, we recall the classical tube-based output feedback control formulation [1, Ch. 5].

A. Observer Design

A Luenberger observer is employed to estimate the state, so that the estimated state dynamics read

$$\hat{x}(k+1) = A\hat{x}(k) + Bu(k) + L(y(k) - C\hat{x}(k)), \tag{3}$$

where the matrix L is such that $A_L \triangleq A - LC$ is Schur. The *estimation error* between the true and estimated state is defined as $\tilde{x}(k) \triangleq x(k) - \hat{x}(k)$ and evolves as

$$\tilde{x}(k+1) = A_L\tilde{x}(k) + \tilde{\delta}(k), \tag{4}$$

where $\tilde{\delta}(k) = w(k) - Ln(k)$, and therefore $\tilde{\delta}(k) \in \tilde{\Delta} \triangleq \mathcal{W} \oplus (-L\mathcal{N})$. Let the initial estimation error $\tilde{x}(0)$ belong to a set $\tilde{\mathcal{S}}_0$. Then, according to (4), $\tilde{x}(k) \in \tilde{\mathcal{S}}(k)$ where the set sequence $\tilde{\mathcal{S}}(k)$ satisfies

$$\tilde{\mathcal{S}}(k+1) = A_L\tilde{\mathcal{S}}(k) \oplus \tilde{\Delta}, \tag{5}$$

with $\tilde{\mathcal{S}}(0) = \tilde{\mathcal{S}}_0$. The observer dynamics in (3) can be rewritten as

$$\hat{x}(k+1) = A\hat{x}(k) + Bu(k) + \delta(k), \tag{6}$$

with $\delta(k) = L(y(k) - C\hat{x}(k)) = LC\tilde{x}(k) + Ln(k)$. Hence, $\delta(k) \in \Delta(k) \triangleq LC\tilde{\mathcal{S}}(k) \oplus L\mathcal{N}$. Note that $\delta(k)$ behaves as a bounded additive process disturbance for the observer state dynamics (6).

B. Controller Design

As usual in tube-based control techniques, the control policy is chosen as

$$u(k) = v(k) + K(\hat{x}(k) - z(k)), \tag{7}$$

where the matrix K is such that $A_K \triangleq A + BK$ is Schur and $z(k)$ satisfies the nominal disturbance-free dynamics

$$z(k+1) = Az(k) + Bv(k). \tag{8}$$

driven by the nominal control signal $v(k)$. The *control error* is defined as $e(k) \triangleq \hat{x}(k) - z(k)$ and its dynamics are obtained by subtracting (8) from (6), thus resulting in

$$e(k+1) = A_K e(k) + \delta(k). \tag{9}$$

Assume the initial control error belongs to a bounded set $\mathcal{S}_0$, then $e(k) \in \mathcal{S}(k)$, where the sequence $\mathcal{S}(k)$ satisfies

$$\mathcal{S}(k+1) = A_K\mathcal{S}(k) \oplus \Delta(k) \tag{10}$$

with $\mathcal{S}(0) = \mathcal{S}_0$. Note that if $\mathcal{S}_0 = \{0\}$, which corresponds to choosing $z(k) = \hat{x}(k)$, then the set sequence $\mathcal{S}(k)$ can be computed as $\mathcal{S}(k) = \sum_{i=0}^{k-1} A_K^i \Delta(k-i-1)$. Let us define the tightened constraints for the nominal system

$$\begin{aligned} z(k) &\in \mathcal{Z}(k) \triangleq \mathcal{X}(k) \ominus \left[\mathcal{S}(k) \oplus \tilde{\mathcal{S}}(k)\right], \\ v(k) &\in \mathcal{V}(k) \triangleq \mathcal{U}(k) \ominus K\mathcal{S}(k). \end{aligned} \tag{11}$$

It turns out that, if the nominal state and input sequences satisfy the tightened constraints (11), then the perturbed trajectories of the closed-loop system (1) with the control law (7) satisfy the state and input constraints (2).

III. Output Feedback VH-MPC

In this work, the nominal control input $v(k)$ in (7) is computed via a VH-MPC scheme. In particular, at each time instant k, the following optimization problem $\mathbb{P}_k(\hat{x}(k), \mathcal{Z}_{f,k})$ is considered

$$\min_{N_k, \boldsymbol{v}_k, \boldsymbol{z}_k} J_k = N_k + \gamma \sum_{j=0}^{N_k-1} \|v_k(j)\| \tag{12a}$$

$$\text{s.t.} \quad z_k(0) = \hat{x}(k) \tag{12b}$$

$$z_k(j+1) = Az_k(j) + Bv_k(j) \tag{12c}$$

$$z_k(j) \in \mathcal{Z}_k(j), \quad j = 1, \dots, N_k - 1 \tag{12d}$$

$$v_k(j) \in \mathcal{V}_k(j), \quad j = 0, \dots, N_k - 1 \tag{12e}$$

$$z_k(N_k) \in \{r(k+N_k)\} \oplus \mathcal{Z}_{f,k} \tag{12f}$$

where the sequences $\boldsymbol{v}_k = [v_k(0), \dots, v_k(N_k-1)]$, $\boldsymbol{z}_k = [z_k(0), \dots, z_k(N_k)]$ are the nominal inputs and states, respectively, along the prediction horizon N_k, and $\|\cdot\|$ indicates an arbitrary vector norm. The solution of $\mathbb{P}_k(x(k), \mathcal{Z}_{f,k})$ consists of the optimal cost J_k^*, the optimal horizon length N_k^*, and the optimal input and state sequences, $\boldsymbol{v}_k^*$ and $\boldsymbol{z}_k^*$, respectively. Note that, given the initial state constraint $z_k(0) = \hat{x}(k)$, the control error $e(k)$ at every time step k is equal to zero and thus the control law (7) can be written as $u(k) = v_k^*(0)$. In (12), the tightened constraints along the prediction horizon are defined as

$$\begin{aligned} \mathcal{Z}_k(j) &\triangleq \mathcal{X}(k+j) \ominus \left[\mathcal{S}_k(j) \oplus \tilde{\mathcal{S}}_k(j)\right], \\ \mathcal{V}_k(j) &\triangleq \mathcal{U}(k+j) \ominus K\mathcal{S}_k(j), \end{aligned} \tag{13}$$

where $\tilde{\mathcal{S}}_k(j) \triangleq \tilde{\mathcal{S}}(k+j)$ and

$$\mathcal{S}_k(j) = \sum_{i=0}^{j-1} A_K^i \Delta_k(j-i-1), \tag{14}$$

and $\Delta_k(j) \triangleq \Delta(k+j) = LC\tilde{\mathcal{S}}_k(j) \oplus L\mathcal{N}$. Notice that (14) corresponds to (10) taking into account that $e(k) = 0$, and hence $\mathcal{S}_k(0) = \{0\}$, at every time step k.

The key ingredient of problem (12) is the terminal constraint set $\mathcal{Z}_{f,k}$, whose design is crucial both for recursive feasibility and to achieve a close proximity to the reference trajectory. This is discussed in the next subsection.

Algorithm 1 OF-ATC Scheme

Input $\hat{x}(0)$, λ
$k \leftarrow 0$
Solve $\mathbb{P}_0(\hat{x}(0), \{0\})$ and get $(J_0^*,\, N_0^*,\, v_0^*,\, z_0^*)$
$u(0) \leftarrow v_0^*(0)$
$\hat{x}(1) \leftarrow A\hat{x}(0) + Bu(0) + L(y(0) - C\hat{x}(0))$
$\mathcal{Z}_{f,0} \leftarrow \{0\}$, $q \leftarrow 0$
while $N_k^* > 1$ **do**
  $k \leftarrow k + 1$
  (C1) Solve $\mathbb{P}_k(\hat{x}(k), \{0\})$, get $(\bar{J}_k^*, \bar{N}_k^*, \bar{v}_k^*, \bar{z}_k^*)$
  if $\bar{J}_k^* > J_{k-1}^* - \lambda$ **then**
    $\mathcal{Z}_{f,k} \leftarrow \mathcal{Z}_{f,k-1} \oplus A_K^{N_{k-1}^*-1}\Delta(k-1)$
    (C2) Solve $\mathbb{P}_k(\hat{x}(k), \mathcal{Z}_{f,k})$ and get $(J_k^*, N_k^*, v_k^*, z_k^*)$
  else
    $(J_k^*, N_k^*, v_k^*, z_k^*) \leftarrow (\bar{J}_k^*, \bar{N}_k^*, \bar{v}_k^*, \bar{z}_k^*)$
    $\mathcal{Z}_{f,k} \leftarrow \{0\}$
    $T_l \leftarrow k$
  end if
  $u(k) \leftarrow v_k^*(0)$
  $\hat{x}(k+1) \leftarrow A\hat{x}(k) + Bu(k) + L(y(k) - C\hat{x}(k))$
end while
return T_l, $T_c \leftarrow k + 1$

A. VH-MPC with Adaptive Terminal Constraints

With the goal of intercepting the reference trajectory $r(k)$, a natural choice for the terminal constraint set would be $\mathcal{Z}_{f,k} = \{0\}$ for all k, resulting in the terminal equality constraint $z_k(N_k) = r(k + N_k)$. However, it turns out that process and measurement disturbances can make this constraint infeasible. To address this issue, we propose a control strategy relying on an adaptive choice of the terminal set $\mathcal{Z}_{f,k}$ that ensures recursive feasibility, finite-time convergence, and minimizes the distance to the desired trajectory.

The approach prioritizes solving problem (12) with the terminal equality constraint $\mathcal{Z}_{f,k} = \{0\}$ as long as it is feasible and the optimal cost decreases by at least a predefined threshold λ compared to the previous step. If this condition is not met, a problem with an expanded terminal set $\mathcal{Z}_{f,k}$ is solved to ensure feasibility and a sufficient cost decrease. More specifically, at each time k, problem $\mathbb{P}_k(\hat{x}(k), \{0\})$ is solved. If its resulting optimal cost $\bar{J}_k^*$ satisfies $\bar{J}_k^* \leq J_{k-1}^* - \lambda$, the control action is computed using this solution, $\mathcal{Z}_{f,k}$ is reset to $\{0\}$, and the algorithm proceeds to the next step. If, conversely, problem $\mathbb{P}_k(\hat{x}(k), \{0\})$ is infeasible or $\bar{J}_k^* > J_{k-1}^* - \lambda$, the problem $\mathbb{P}_k(x(k), \mathcal{Z}_{f,k})$ is solved instead, with the terminal set defined as

$$\mathcal{Z}_{f,k} = \mathcal{Z}_{f,k-1} \oplus A_K^{N_{k-1}^*-1}\Delta(k-1). \tag{15}$$

The solution of this problem is then used for selecting the control action at time k. The entire procedure of the proposed Output Feedback VH-MPC with Adaptive Terminal Constraints (hereafter denoted as OF-ATC) is detailed in Algorithm 1. The following assumption is enforced in order to ensure that there exists an initial feasible control sequence (of any length).

Assumption 1: The problem $\mathbb{P}_0(\hat{x}(0), \{0\})$ is feasible.

The following result establishes the key properties of the proposed scheme.

Theorem 1: Let Assumption 1 be satisfied. Then, the following statements hold:

(i) Problems $\mathbb{P}_k(\hat{x}(k), \mathcal{Z}_{f,k})$, where the sets $\mathcal{Z}_{f,k}$ are defined according to Algorithm 1, are feasible for all $k = 1, 2, \ldots$ and any $w(k) \in \mathcal{W}$ and $n(k) \in \mathcal{N}$;

(ii) By selecting γ in the cost J_k such that

$$\bar{\lambda} \triangleq 1 - \gamma \sup_k \left\{ \sup_{\delta \in \Delta(k)} \sum_{j=0}^{\infty} \|KA_K^j \delta\| \right\} > 0, \tag{16}$$

and setting $\lambda = \bar{\lambda}$ in Algorithm 1, the optimal cost decreases by at least $\bar{\lambda}$ at each step, i.e.

$$J_{k+1}^* \leq J_k^* - \bar{\lambda}, \, \forall k. \tag{17}$$

Proof: (i) At step k, the solution $\boldsymbol{v}_k^*$, $\boldsymbol{z}_k^*$ results from problem $\mathbb{P}_k(\hat{x}(k), \mathcal{Z}_{f,k})$, with $\mathcal{Z}_{f,k}$ chosen as in Algorithm 1. Feasibility of this problem implies that

$$z_k^*(0) = \hat{x}(k) \tag{18}$$
$$z_k^*(j) \in \mathcal{Z}_k(j), \quad j = 1, \ldots, N_k^* - 1 \tag{19}$$
$$v_k^*(j) \in \mathcal{V}_k(j), \quad j = 0, \ldots, N_k^* - 1 \tag{20}$$
$$z_k^*(j+1) = Az_k^*(j) + Bv_k^*(j), \quad j = 0, \ldots, N_k^* - 1 \tag{21}$$
$$z_k^*(N_k^*) \in \{r(k + N_k^*)\} \oplus \mathcal{Z}_{f,k}, \tag{22}$$

where $\mathcal{Z}_k(j)$ and $\mathcal{V}_k(j)$ are defined in (13). Consider now the candidate solution $\boldsymbol{v}'_{k+1}$, $\boldsymbol{z}'_{k+1}$ for step $k+1$ with length $N_k^* - 1$, defined as follows

$$\begin{aligned} z'_{k+1}(j) &= z_k^*(j+1) + A_K^j \delta(k), \quad j = 0, \ldots, N_k^* - 1 \\ v'_{k+1}(j) &= v_k^*(j+1) + KA_K^j \delta(k), \quad j = 0, \ldots, N_k^* - 2, \end{aligned} \tag{23}$$

where $\delta(k)$ depends on the realizations of $w(k)$ and $n(k)$. In the following, we prove the feasibility of the candidate solution (23) for the problem $\mathbb{P}_{k+1}(\hat{x}(k+1), \mathcal{Z}_{f,k+1})$. In particular, we show that constraints (12b)-(12f) are satisfied by the candidate solution (23) at step $k+1$. First, by exploiting (18), (23) and the closed-loop observer dynamics, one has

$$\begin{aligned} z'_{k+1}(0) &= z_k^*(1) + LC\tilde{x}(k) + Ln(k) \\ &= Az_k^*(0) + Bv_k^*(0) + LC\tilde{x}(k) + Ln(k) \\ &= A\hat{x}(k) + Bu(k) + LC\tilde{x}(k) + Ln(k) = \hat{x}(k+1). \end{aligned}$$

Hence the initial constraint (12b) is satisfied by $z'_{k+1}(0)$. From (21), one has that

$$z_k^*(j+2) = Az_k^*(j+1) + Bv_k^*(j+1). \tag{24}$$

By using (23), equation (24) can be written as

$$\begin{aligned} z_k^*(j+2) &= z'_{k+1}(j+1) - A_K^{j+1}\delta(k) \\ &= A\left(z'_{k+1}(j) - A_K^j \delta(k)\right) + B\left(v'_{k+1}(j) - KA_K^j \delta(k)\right) \\ &= Az'_{k+1}(j) + Bv'_{k+1}(j) - A_K^{j+1}\delta(k). \end{aligned}$$

Hence, $z'_{k+1}(j+1) = Az'_{k+1}(j) + Bv'_{k+1}(j)$ and thus $\boldsymbol{z}'_{k+1}, \boldsymbol{v}'_{k+1}$ satisfies (12c). Using (19)-(23) and (13), one has

$$\begin{aligned} z'_{k+1}(j) &\in \mathcal{Z}_k(j+1) \oplus A_K^j \Delta(k) \\ &= \mathcal{X}(k+j+1) \ominus \left[\mathcal{S}_k(j+1) \oplus \tilde{\mathcal{S}}_k(j+1)\right] \oplus A_K^j \Delta(k) \\ &= \mathcal{X}(k+j+1) \ominus \left[\sum_{i=0}^{j} A_K^i \Delta_k(j-i) \oplus \tilde{\mathcal{S}}_k(j+1)\right] \oplus A_K^j \Delta(k). \end{aligned}$$

Then, by (14) and recalling that $\Delta_k(0) = \Delta(k)$ and $\tilde{\mathcal{S}}_k(j+1) = \tilde{\mathcal{S}}_{k+1}(j)$, one gets

$$\begin{aligned} z'_{k+1}(j) &\in \mathcal{X}(k+j+1) \ominus \left[\sum_{i=0}^{j-1} A_K^i \Delta_k(j-i-1) \oplus \tilde{\mathcal{S}}_{k+1}(j)\right] \\ &= \mathcal{X}(k+j+1) \ominus \left[\mathcal{S}_{k+1}(j) \oplus \tilde{\mathcal{S}}_{k+1}(j)\right] = \mathcal{Z}_{k+1}(j) \end{aligned}$$

and hence the sequence $\boldsymbol{z}'_{k+1}$ satisfies (12d). Proving that $\boldsymbol{v}'_{k+1}$ satisfies (12e) follows a similar argument. Finally, the terminal state of the candidate solution (23), satisfies:

$$\begin{aligned} z'_{k+1}(N_k^* - 1) &= z_k^*(N_k^*) + A_K^{N_k^*-1}\delta(k) \\ &\in \{r(k+N_k^*)\} \oplus \mathcal{Z}_{f,k} \oplus A_K^{N_k^*-1}\Delta(k) \\ &= \{r(k+N_k^*)\} \oplus \mathcal{Z}_{f,k+1}, \end{aligned}$$

where $\mathcal{Z}_{f,k}$ is defined as in Algorithm 1. Hence, $z'_{k+1}(N_k^*-1)$ satisfies the terminal constraint (12f). This concludes the proof of recursive feasibility.

(ii) If $\bar{J}_{k+1}^* \leq J_k^* - \bar{\lambda}$, (17) holds by construction. Otherwise, by using (16), it is easy to show that the cost J'_{k+1} associated to the candidate solution (23) is such that $J'_{k+1} \leq J_k^* - \bar{\lambda}$. Since the optimal solution of problem $\mathbb{P}_{k+1}(x(k+1), \mathcal{Z}_{f,k+1})$ clearly satisfies $J_{k+1}^* \leq J'_{k+1}$, (17) immediately follows. ∎

Remark 1: The computation of $\bar{\lambda}$ in (16) can be demanding, even though it is performed offline. Nevertheless, the complexity can be mitigated as follows. First, concerning the infinite summation in (16), the terms $\|KA_K^j\delta\|$ decay exponentially to zero as $j \to \infty$. Consequently, the summation can be truncated after a sufficiently large number of terms, without significant loss of accuracy. The most computationally intensive part is the evaluation of the inner supremum over the set $\Delta(k)$. In general, if the sets $\mathcal{W}$, $\mathcal{N}$ and $\tilde{\mathcal{S}}_0$ are polytopes, also $\Delta(k)$ is a polytope, whose number of facets and vertices grows with k. In order to reduce the computational burden, one may assume that $\mathcal{W}$, $\mathcal{N}$ and $\tilde{\mathcal{S}}_0$ are zonotopes, which implies that $\Delta(k)$ is a zonotope itself [17]. While the exact propagation of $\Delta(k)$ becomes trivial, the number of its vertices still grows exponentially with the number of zonotope generators. However, it is possible to limit the number of vertices by computing a zonotope containing $\Delta(k)$ with a prescribed maximum number of generators. This can be done by using one of the available techniques for zonotope order reduction [18].

The next result defines the convergence properties of the proposed control scheme.

Theorem 2: Let Assumption 1 be satisfied. Then, the trajectories $\hat{x}(k)$ of the observer (3), with the VH-MPC control law defined via Algorithm 1, converge in a finite number of steps T_c to the set

$$\hat{\mathcal{T}} = \{r(T_c)\} \oplus \sum_{i=T_l}^{T_c-1} A_K^{N_i^*-1}\Delta(i), \tag{25}$$

with T_l as returned by Algorithm 1. The trajectories $x(k)$ of the closed-loop system (1) with the VH-MPC control law converge to the set

$$\mathcal{T} = \hat{\mathcal{T}} + \tilde{\mathcal{S}}(T_c). \tag{26}$$

Moreover, $T_c \leq \lfloor J_0^*/\bar{\lambda} \rfloor$ where J_0^* is the optimal cost of the initial problem $\mathbb{P}_0(\hat{x}(0), \{0\})$.

Proof: The cost decrease condition (17) guarantees that Algorithm 1 terminates in a number of steps $T_c \leq \lfloor J_0^*/\bar{\lambda} \rfloor$. Moreover, at step $k = T_c - 1$, the optimization problem $\mathbb{P}_{T_c-1}(\hat{x}(T_c-1), \mathcal{Z}_{f,T_c-1})$ is solved with the terminal set

$$\mathcal{Z}_{f,T_c-1} = \sum_{i=T_l}^{T_c-2} A_K^{N_i^*-1}\Delta(i),$$

being T_l the time step in which the control action is selected for the last time as the solution of problem $\mathbb{P}_k(\hat{x}(k), \{0\})$ during the execution of Algorithm 1. Then, since $N_{T_c-1}^* = 1$ by construction (see line 7 of Algorithm 1), the final observer state is $\hat{x}(T_c) = z_{T_c-1}^*(1) + \delta(T_c-1)$ and then, by (12f)

$$\hat{x}(T_c) \in \{r(T_c)\} \oplus \mathcal{Z}_{f,T_c-1} \oplus \Delta(T_c-1) = \hat{\mathcal{T}}.$$

Finally, (26) follows from $x(T_c) = \hat{x}(T_c) + \tilde{x}(T_c)$ and $\tilde{x}(T_c) \in \tilde{\mathcal{S}}(T_c)$. ∎

Remark 2: The proposed VH-MPC control scheme can be easily extended to a setting in which the reference trajectory $r(k)$ is not known exactly. In fact, if it is assumed that $r(k) \in \mathcal{R}(k)$, where $\mathcal{R}(k)$ is a sequence of bounded convex sets, one just has to replace the singleton $\{r(\cdot)\}$ with the set $\mathcal{R}(\cdot)$ in the terminal constraint (12f) and in the subsequent technical developments. In this way, the properties of the control scheme established in Theorems 1 and 2 still hold.

Remark 3: The proposed control law does not impose specific assumptions on the reference trajectory $r(k)$. However, the feasibility of problem $\mathbb{P}_0(\hat{x}(k), \{0\})$ (Assumption 1) implicitly depends on $r(k)$. In particular, the characteristics of $r(k)$ influence the range of feasible horizon lengths N_k, which in turn affects the flexibility of the VH-MPC scheme.

B. Properties of OF-ATC

The proposed approach presents several novel features that make it different from other existing methods. First, it has been observed that the solution of problem $\mathbb{P}_k(\hat{x}(k), \{0\})$ satisfies the cost decrease condition $\bar{J}_k^* \leq J_{k+1}^* - \bar{\lambda}$ for most of the time, and thus problem $\mathbb{P}_k(\hat{x}(k), \mathcal{Z}_{f,k})$ with $\mathcal{Z}_{f,k} \neq \{0\}$ is solved only for very few consecutive steps right before maneuver completion. Consequently, the set $\hat{\mathcal{T}}$ defined in (25), is usually the sum of very few terms. This leads to a small convergence set around the selected point on the reference trajectory, thus reducing the final distance to the target if compared to more conservative methods in which the terminal constraint set sequence is fixed a priori (see, e.g, [9]).

Unlike the receding-horizon techniques described in [13], the proposed method does not require the initial sets $\tilde{\mathcal{S}}_0$ and $\mathcal{S}_0$ to be robustly positive invariant (RPI) with respect to $\tilde{\delta}(k)$ and $\delta(k)$ for the systems (4) and (6), respectively.

Finally, it is worth observing that Assumption 1 is less conservative than the usual assumption made in standard tube-based MPC, which requires the feasibility of the initial optimization problem for a pre-defined fixed horizon length. Indeed, Assumption 1 only requires that the initial optimization problem $\mathbb{P}_k(\hat{x}(k), \{0\})$ is feasible for some horizon length, thus increasing the flexibility of the control scheme.

IV. Simulation Results

The effectiveness of the proposed control law is tested on an orbital rendezvous between a controlled spacecraft and an uncontrolled tumbling object, which is relevant in applications such as active debris removal [19], [20].

The dynamics of the controlled spacecraft are governed by the Hill-Clohessy-Wiltshire (HCW) equations [21], formulated in the radial-transverse-normal frame centered at the target center of mass. These equations are discretized with sampling time $t_s = 11.7$ s. The state vector $x(k) = \left[x_p^T(k)\ x_v^T(k)\right]^T$ includes the spacecraft position and velocity vectors. The control input $u(k)$ is the acceleration vector. Only measurements of the position $x_p(k)$ are assumed to be available, corrupted by noise $n(k) \in \mathcal{N} = [-0.01, 0.01]^3$ m. The spacecraft dynamics are assumed to be affected by a bounded process disturbance $w(k) \in \mathcal{W} = \left[-2 \cdot 10^{-3}, 2 \cdot 10^{-3}\right]^3$ m $\times$ $\left[10^{-3}, 10^{-3}\right]^3$ m/s.

The target object is tumbling with a period of 600 s around a spin axis orthogonal to the orbital plane. Its docking port is located 1.5 m from the center of mass, while the capture point is situated at a distance of 2 m. The reference trajectory $r(k) = \left[z_p^r(k)^T\ z_v^r(k)^T\right]^T$ is given by position and velocity of the capture point and can be computed from the trajectory of the docking port $x^d(k) = \left[x_p^d(k)^T\ x_v^d(k)^T\right]^T$. These trajectories are obtained by integrating the rotational kinematics of a rigid body and sampled at intervals of t_s.

The spacecraft is required to remain within a visibility cone stemming from the docking port with a half-angle $\alpha = 30$ deg. In this work, the cone is approximated with a polytopic inner approximation. Moreover, the control input must satisfy $\|u(k)\|_\infty \leq 0.02$ m/s^2. These requirements define the time-varying constraint sets $\mathcal{X}(k), \mathcal{U}$ in (2). Figure 1 provides a schematic representation of the considered scenario. For further details, the reader is referred to [22].

The maximum initial estimation error on the position and velocities are 0.2 m and 10^{-4} m/s, respectively, thus $\tilde{\mathcal{S}}_0$ in (5) is a box. It is important to note that this set is not RPI for system (4) with respect to $\tilde{\delta}(k)$. The control effort in the cost J_k is weighted in the 1-norm (which accounts for fuel consumption) with $\gamma = 3$, corresponding to $\bar{\lambda} = 0.29$ in (16). In this case study, $\bar{\lambda}$ has been computed by taking the sup in (16) over a box containing $\Delta(k)$ (as explained in Remark 1).

A Monte Carlo simulation across 100 different scenarios satisfying Assumption 1 has been conducted. For each scenario, the initial radial and transverse coordinates of the spacecraft

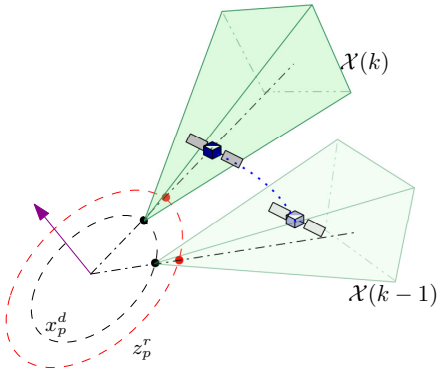

Fig. 1. Qualitative illustration of the rendezvous mission. The capture point trajectory $\boldsymbol{z_p^r(k)}$ is depicted in dashed-red, while the docking port position $\boldsymbol{x_p^d(k)}$ in dashed-black. The green sets are the visibility cones and the purple arrow is the spin axis. The dashed-blue line is the trajectory $\boldsymbol{x_p(k)}$.

are uniformly sampled over $[-50, -15]$ m and $[-10, 10]$ m, respectively, with the initial normal position and velocity vector set equal to zero. The initial estimation error $\tilde{x}(0)$ has been sampled from $\tilde{\mathcal{S}}_0$. The disturbance sequences $w(k)$ and $n(k)$ used in all experiments have been uniformly sampled from the sets $\mathcal{W}$ and $\mathcal{N}$, respectively.

In the 100 tests, the average final distance to the capture point is 0.04 m and the average final velocity error is 0.001 m/s. The average value of $T_c - T_l$, corresponding to the number of terms in the sum in (25) is 2.04 (96% of the occurrences are equal to 2). This confirms that the final set $\hat{\mathcal{T}}$ is typically small, thus ensuring a close proximity of the final state to the reference trajectory. The simulations have been performed in MATLAB on a laptop equipped with an Intel Core i7-1165G7 and 16 GB of RAM. Each instance of problem (12) is solved by enumerating over a finite set of prediction horizons, $N_k \in \{1, \ldots, 30\}$, leading to a corresponding finite set of linear programs (LPs). Each LP is solved using the Gurobi optimizer. The average execution time is 0.5 s, which is much smaller than the selected t_s.

The performance of the OF-ATC algorithm has been first compared to a control scheme with a pre-defined (non adaptive) terminal constraint sequence. In particular, at each time step k, problem (12) is solved with the terminal constraint set chosen as $\mathcal{Z}_{f,k} = \mathcal{Q} \ominus \left[\mathcal{S}_k(N_k) \oplus \tilde{\mathcal{S}}_k(N_k)\right]$, with $\mathcal{Q} = \mathcal{S}(\infty) \oplus \tilde{\mathcal{S}}(\infty)$ (computed as described in [23]). This corresponds to the control law in [9] adapted to the output feedback setting, and guarantees that the state trajectories terminate in the set $\mathcal{Q}$. This control scheme achieves an average final position error of 0.52 m and a final velocity error of 0.011 m/s, which are approximately one order of magnitude larger than those obtained using OF-ATC. Moreover, the minimum distance is more than 4 times larger than the maximum distance achieved by OF-ATC. A comparison on the resulting trajectories for one simulation is reported in Fig. 2, together with the final sets ensured by the two control laws. These results highlight the reduced conservatism of the proposed approach, thanks to the adaptive mechanism for the selection of the terminal constraint.

Additionally, the performance of OF-ATC has been evaluated against its state-feedback version in [10] (denoted as SF-

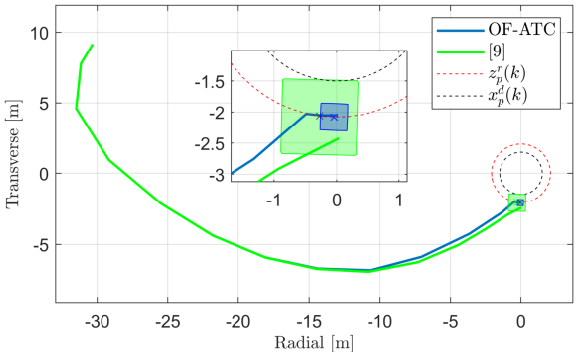

Fig. 2. Trajectories $\boldsymbol{x_p(k)}$ resulting from OF-ATC (blue) and the control law borrowed from [9] (green). The set $\boldsymbol{\mathcal{T}}$ is depicted in blue, while the green set is $\boldsymbol{\mathcal{Q}}$. The points $\boldsymbol{z_p^r(T_c)}$ for the two laws are the blue and green crosses. The whole reference $\boldsymbol{z_p^r(k)}$ and docking port $\boldsymbol{x_p^d(k)}$ trajectories are reported in dashed-red and dashed-black, respectively.

ATC), in which the full state is assumed to be exactly known. This comparison aims to assess the performance degradation introduced by output feedback with noisy measurements. The results indicate that the final distance achieved by SF-ATC is approximately 5 times smaller, while the control effort is reduced by a factor of 1.25. No significant differences are observed in terms of completion time. On the other hand, if noisy position measurements (along with exact velocity measurements) are fed to the SF-ATC scheme, feasibility is lost during the maneuver in 49 cases, due to state constraint violations. The performance drop exhibited by OF-ATC is justified by the necessity to deal with partial state information and to compensate for measurement noise.

Finally, the receding-horizon control law proposed in [13] has been tested on the same scenario with fixed prediction horizon equal to 30. Recall that this control law requires $\mathcal{S}(0)$ and $\tilde{\mathcal{S}}(0)$ to be RPI sets for systems (9) and (4) with respect to $\delta(k)$ and $\tilde{\delta}(k)$, respectively. Therefore, they cannot be smaller that the minimal RPI sets $\mathcal{S}(\infty)$ and $\tilde{\mathcal{S}}(\infty)$. However, these sets are generally large and, consequently, they may lead to a severe constraint tightening. Indeed, when the minimal RPI sets are chosen to initialize the receding-horizon MPC, none of the 100 tested scenarios is initially feasible. This confirms the higher flexibility of the variable-horizon approach.

V. Conclusions

This letter presented a robust output feedback variable-horizon MPC framework for intercepting a moving target in the presence of bounded process disturbances and measurement noise. The proposed approach relies on an adaptive mechanism for setting the terminal set of the MPC optimization problem, which allows one to reduce significantly the final distance to the target, as demonstrated through numerical simulations on an orbital rendezvous maneuver with a tumbling target. Future work will focus on the use of set membership state estimation techniques, in combination with the VH-MPC control scheme, and on the extension of the proposed approach to nonlinear systems.

References

[1] J. B. Rawlings, D. Q. Mayne, and M. Diehl, *Model predictive control: theory, computation, and design*, vol. 2. Nob Hill Publishing Madison, WI, 2017.
[2] L. Van den Broeck, M. Diehl, and J. Swevers, "A model predictive control approach for time optimal point-to-point motion control," *Mechatronics*, vol. 21, no. 7, pp. 1203–1212, 2011.
[3] C. Rösmann, F. Hoffmann, and T. Bertram, "Timed-elastic-bands for time-optimal point-to-point nonlinear model predictive control," in *2015 european control conference (ECC)*, pp. 3352–3357, IEEE, 2015.
[4] R. Verschueren, H. J. Ferreau, A. Zanarini, M. Mercangöz, and M. Diehl, "A stabilizing nonlinear model predictive control scheme for time-optimal point-to-point motions," in *2017 IEEE 56th annual conference on decision and control (CDC)*, pp. 2525–2530, IEEE, 2017.
[5] A. J. Krener, "Adaptive horizon model predictive control," *IFAC-PapersOnLine*, vol. 51, no. 13, pp. 31–36, 2018.
[6] R. L. Sutherland, I. V. Kolmanovsky, A. R. Girard, F. A. Leve, and C. D. Petersen, "On closed-loop Lyapunov stability with minimum-time MPC feedback laws for discrete-time systems," in *2019 IEEE 58th Conference on Decision and Control (CDC)*, pp. 5231–5237, IEEE, 2019.
[7] W. B. Greer and C. Sultan, "Shrinking horizon model predictive control method for helicopter–ship touchdown," *Journal of Guidance, Control, and Dynamics*, vol. 43, no. 5, pp. 884–900, 2020.
[8] H. Farooqi, L. Fagiano, P. Colaneri, and D. Barlini, "Shrinking horizon parametrized predictive control with application to energy-efficient train operation," *Automatica*, vol. 112, p. 108635, 2020.
[9] A. Richards and J. P. How, "Robust variable horizon model predictive control for vehicle maneuvering," *International Journal of Robust and Nonlinear Control*, vol. 16, no. 7, pp. 333–351, 2006.
[10] R. Quartullo, G. Bianchini, A. Garulli, and A. Giannitrapani, "Robust variable-horizon MPC with adaptive terminal constraints," *arXiv preprint arXiv:2410.08807*, 2024.
[11] D. Q. Mayne, S. V. Raković, R. Findeisen, and F. Allgöwer, "Robust output feedback model predictive control of constrained linear systems," *Automatica*, vol. 42, no. 7, pp. 1217–1222, 2006.
[12] M. Kögel and R. Findeisen, "Robust output feedback MPC for uncertain linear systems with reduced conservatism," *IFAC-PapersOnLine*, vol. 50, no. 1, pp. 10685–10690, 2017.
[13] D. Q. Mayne, S. Raković, R. Findeisen, and F. Allgöwer, "Robust output feedback model predictive control of constrained linear systems: Time varying case," *Automatica*, vol. 45, no. 9, pp. 2082–2087, 2009.
[14] L. Chisci and G. Zappa, "Feasibility in predictive control of constrained linear systems: the output feedback case," *International Journal of Robust and Nonlinear Control: IFAC-Affiliated Journal*, vol. 12, no. 5, pp. 465–487, 2002.
[15] F. D. Brunner, M. A. Müller, and F. Allgöwer, "Enhancing output-feedback MPC with set-valued moving horizon estimation," *IEEE Transactions on Automatic Control*, vol. 63, no. 9, pp. 2976–2986, 2018.
[16] Z. Dong and D. Angeli, "Homothetic tube-based robust economic MPC with integrated moving horizon estimation," *IEEE Transactions on Automatic Control*, vol. 66, no. 1, pp. 64–75, 2020.
[17] M. Althoff and B. H. Krogh, "Zonotope bundles for the efficient computation of reachable sets," in *2011 50th IEEE conference on decision and control and European control conference*, pp. 6814–6821, IEEE, 2011.
[18] X. Yang and J. K. Scott, "A comparison of zonotope order reduction techniques," *Automatica*, vol. 95, pp. 378–384, 2018.
[19] M. Shan, J. Guo, and E. Gill, "Review and comparison of active space debris capturing and removal methods," *Progress in Aerospace Sciences*, vol. 80, pp. 18–32, 2016.
[20] M. Leomanni, G. Bianchini, A. Garulli, A. Giannitrapani, and R. Quartullo, "Orbit control techniques for space debris removal missions using electric propulsion," *Journal of Guidance, Control, and Dynamics*, vol. 43, no. 7, pp. 1259–1268, 2020.
[21] W. Clohessy and R. Wiltshire, "Terminal guidance system for satellite rendezvous," *Journal of the aerospace sciences*, vol. 27, no. 9, pp. 653–658, 1960.
[22] M. Leomanni, R. Quartullo, G. Bianchini, A. Garulli, and A. Giannitrapani, "Variable-horizon guidance for autonomous rendezvous and docking to a tumbling target," *Journal of Guidance, Control, and Dynamics*, vol. 45, no. 5, pp. 846–858, 2022.
[23] S. V. Rakovic, E. C. Kerrigan, K. I. Kouramas, and D. Q. Mayne, "Invariant approximations of the minimal robust positively invariant set," *IEEE Transactions on automatic control*, vol. 50, no. 3, pp. 406–410, 2005.